Available online at www.sciencedirect.com

ScienceDirect

Procedia CIRP 136 (2025) 111–116

www.elsevier.com/locate/procedia

35th CIRP Design 2025

Enhancement of accuracy in deformation and load estimation of gentelligent, sensor-integrating components for technical inheritance

Sören Meyer zu Westerhausen[a]*, Vaclav Kasal[a], Johanna Wurst[a], Roland Lachmayer[a]

[a]*Institute for Product Development, Leibniz University Hannover, An der Universität 1, 30823 Garbsen, Germany*

* Corresponding author. Tel.: +49 (0)511 762 13356; *E-mail address:* meyer-zu-westerhausen@ipeg.uni-hannover.de

Abstract

The integration of sensors into load-carrying structural, so-called gentelligent, components allows to get insights into load histories during the product use phase. This data enables optimisations of the structure for adaptions on the operational loads. An easy way to reconstruct deformations and loads from measurements at discrete sensor positions on beam-like structures, like an aircraft wing box, is Ko's displacement theory, which suffers from inaccuracies due to needed assumptions when complicated free-form geometries are considered. Therefore, this paper presents an algorithmic solution to enhance the accuracy of this reconstruction by calculating geometric parameters from CAD models for this purpose.

Keywords: Sensor integration; Shape sensing; CAD geometry model; Geometric parameter estimation

1. Introduction

During the last years, a trend to bigger structural components, e. g. due to integral design with composite materials could be observed. On the other hand, for electronic devices, a contrary trend is observable since there is a trend to smaller electronic and measurement components [1].

Nomenclature

ANN	Artificial Neural Network
MM	Modal Method
OSP	Optimal Sensor Placement
iFEM	inverse Finite Elements Method
c_i	Distance to the neutral axis
ε_i	Strain at sensor position i
Δl_i	Distance between two sensors
$tan\,\theta_i$	Slope of the bending line
w_i	Deflection in z-direction
$\%ERMS$	Percentage root mean square error

Besides these trends, there is an increasing need for components with sensory properties, which leads to sensor-integrated components [2,3]. Using the trend of smaller sensors as electronic devices allows the integration of such sensors directly into components while having a minimal invasive influence on mechanical properties. This is especially of interest when composite materials are used where sensor integration into the layup allows the monitoring of the structural behaviour [4]. Data on the structural behaviour and therefore on the operational loads during the use-phase of such sensor-integrating components could not only be used in structural health monitoring, for example for damage detection [5], but also in the product development for optimising the next product generation as an adaption to these loads. Since the sensors become an integral part of the component due to the integration directly into the material, the information on operational loads is "inherited" from one generation to the next, allowing a continuous optimisation in product development over the generations. Therefore, sensor-integrating components are called "gentelligent" in the paradigm of technical inheritance [6,7].

2212-8271
10.1016/j.procir.2025.08.021

If these components are of large-scale, it is necessary to consider a high quantity of sensors which are forming a sensor network. Because of increasing material and manufacturing costs when a high number of sensors has to be integrated into a component, an optimal sensor placement (OSP) is necessary, which minimises both, the sensor quantity and measurement errors in the sensor network [8–10]. Especially when the purpose of the reconstruction of loads and deformations from strain measurements at discrete positions on a part (so-called shape sensing) is considered, the minimisation of measurement errors is highly dependent on the chosen shape sensing method and the assumptions made for their application [11]. Therefore, this paper aims to present an approach to enhance the accuracy of an established shape sensing method for more accurate calculations during the OSP.

For the scope of this paper, it is organised as follows. Section 2 will give an overview of related works by briefly describing the established shape sensing methods and comparing them for further consideration in this paper. From the comparison in Section 2, one method is chosen based on defined criteria, e. g. the possibility to yield results of high accuracy with a reasonable sensor quantity, and the methodology for the enhancement of the calculation accuracy is presented in Section 3. This methodology is then implemented in an algorithmic solution and applied in a case study in Section 4. Last, Section 5 concludes this paper and gives an outlook on future works.

2. Related works

In this section, the established shape sensing methods are presented. Building up on this, it is discussed how they are implemented and in different related works and compared regarding their suitability for this work.

2.1. Shape sensing methods

The reconstruction of deformations from strain measurements as so-called shape sensing is well known and part of different studies in the literature. Established methods can be clustered into four groups in accordance to Gherlone et al. 2018 [12], which will be used as structure to present representative methods in the following. The first group includes methods based on the numerical integration of experimental strains. In the second group, methods using global or piecewise continuous basis functions to approximate the displacement field could be found. Methods employing Artificial Neural Networks (ANN) are forming the fourth group and methods based on a finite-element discrete variational principle the fifth group [12].

A method from the first group, which receives a lot of attention in literature is Ko's displacement theory, which relies on the Euler-Bernoulli beam theory and is therefore well suited for shape sensing of beam-like structures [13]. Therefore, it is applied by Esposito et al. 2020 [11] on the example of an airplane wing box and by Valoriani et al. 2022 [11,14] on the example of an unmanned aerial vehicle's wing. In both works it becomes quite clear that Ko's displacement theory allows a deformation reconstruction with a high accuracy in the principal displacement direction, which is in this case the bending direction, but has poor accuracy in other directions. This is because deformations are only calculated along lines, where the sensors are applied and deformations in other directions are calculated from distortions between the "measurement lines". However, it was observed that there are only comparatively few sensors sensor needed for high accuracy in the bending direction, which is a major advantage. Besides, the calculation is not dependent on material parameters like the Youngs modulus, as long as there are only deformations and no loads calculated [15].

Regarding the second group of methods, especially the Modal Method (MM) gained interest in literature. This method relies on the use of modal transformation, where strains and displacements are expressed in terms of modal coordinates. For this, knowledge of the mode shapes of a component under load is required [12]. In the work of Esposito et al. [11] in which different shape sensing techniques are benchmarked after an OSP, the MM showed results comparable to the results observed with Ko's displacement theory. But in contrast, MM required a significantly higher number of sensors. So, simple strain gauges might not be suitable for this method and fibre optical sensors (FOS) are needed, which requires additional effort for ban planning before the application [16]. Furthermore, MM required a numerical mesh, like from a finite elements method (FEM) simulation, which is not needed in the case of Ko's displacement theory.

Methods in the third group, using ANN, are mostly applied to the deformation reconstruction of frame structures [17]. Especially during the last years, an increasing interest in methods based on ANN could be observed due to the establishment of physics-informed neural networks (PINN). This results from the reduced dependency on training data, which is the most important disadvantage of classical ANN [18,19]. However, in literature there is a lack of studies regarding the needed sensor quantity for accurate calculation results.

The most known and most often applied method for shape sensing is found in the fourth group. It is a method based on specific element definitions, where strain sensors are assumed to be placed on certain elements in a FE mesh and is therefore referred to as inverse FEM (iFEM) [20]. This method was applied for example by Esposito et al. in 2021 for load field reconstruction besides the deformation field reconstruction and was found to be of high accuracy in both applications [21,22]. But a drawback of this method is a not realisable high amount of sensors needed, so there is also a need for FOS [11,23].

2.2. Comparison of the presented methods

The above-described methods show various advantages and disadvantages when it comes to comparison. Table 1 shows a comparison regarding four comparison criteria, using the Harvey balls analysis for the corresponding exemplary publications mentioned before. These criteria are defined by the applicability in real-world applications with strain gauges for measurements. The first criterion (C1) is the need for a high

accuracy when it comes to the reconstruction of load and deformation fields. Second, high accuracy should be achieved by as few sensors as possible (C2) to save costs for material and installation as well as to reduce the computational effort and data management needed to deal with the amount of data. Besides, a simple implementation (C3) is of great importance to allow easy use without a high number of required program scripts. Last, the fourth criterion (C4) is the need to make no assumptions during calculation, for example regarding material or part characteristics, to achieve the most accuracy of results, since assumption could lead to high deviations between reality and reconstructed field information.

Table 1. Comparison of the shape sensing methods for fulfilment of needed characteristics for this study.

Methods / Criteria	Ko Valoriani et al. 2022	MM Esposito et al. 2020	iFEM Esposito et al. 2021	ANN Qui et al. 2023
C1	◑	◑	●	●
C2	●	◑	○	-
C3	●	◑	◑	○
C4	○	●	●	●

Legend: ○ Not fulfilled, ◑ Partly fulfilled, ● Completely fulfilled, - No information available

Regarding the accuracy of results (C1), iFEM and ANN are outperforming the other methods due to their reduced accuracy in other than the principal deformation direction. However, this high accuracy yields the not fulfilled C2 because of the high required sensor quantities. Ko's displacement theory is, besides, superior to the other methods when it comes to implementation since the equations are easy to implement (C3). A major drawback of Ko's displacement theory is the need to make assumptions about the geometric characteristics of the considered component (C4). For example, only beam-like structures could be considered. Furthermore, it becomes clear in the work of Valoriani et al. 2022 [14] that there are assumptions needed when a component with freeform geometry, like an airplane wing, is considered with a tapered cross-section. In their work, for example, there was a need to assume the distance of sensors to the neutral axis of the wing under bending load for the calculation. For simplification, sections were defined where the neutral axis is assumed to be constant, like the exemplary depicted in Fig. 1 for a rectangular tube as a tapered beam.

In this sketch, four cross sections are defined and the parts' hight decreases linearly between two cross sections. Each of the coloured planes shows a part of the component, where the position of the neutral axis is assumed as constant in the approach of [14]. Therefore, this approach is referred to as plane-based approach in the following. The gaps in the vertical distance between each plane to the one of the next sections make clear that this approach results in inaccuracies due to the assumptions made.

To address this issue, there is a need for an algorithmic approach to enhance the accuracy of calculations based on Ko's displacement theory since it shows advantages regarding C2 and C3 and is well suited when load cases with bending and negligible distortion are considered. Therefore, an approach is proposed in the following, to enhance the accuracy with an algorithmic solution which makes assumptions on geometric characteristics unnecessary.

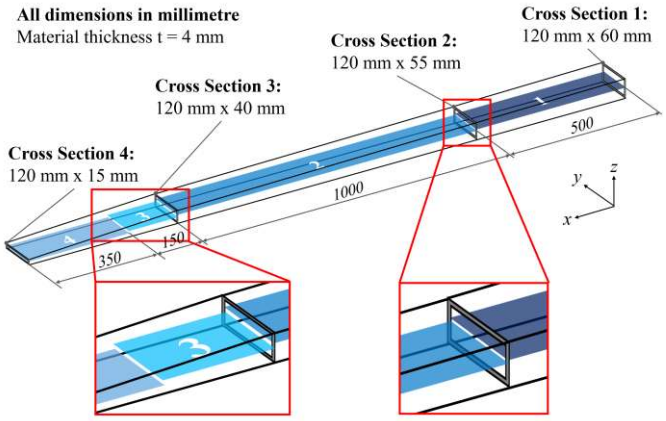

Fig. 1. Sketch of the plane-based approach of (Valoriani et al., 2022) with assumptions on sections with constant neutral axis.

3. Approach for estimating geometric component characteristics

Addressing the issue identified in Section 2, an algorithmic approach is developed to estimate the geometric characteristics on sensor positions on a component for shape sensing with Ko's displacement theory. For a better explanation, the procedure of the algorithm is depicted in Fig. 2.

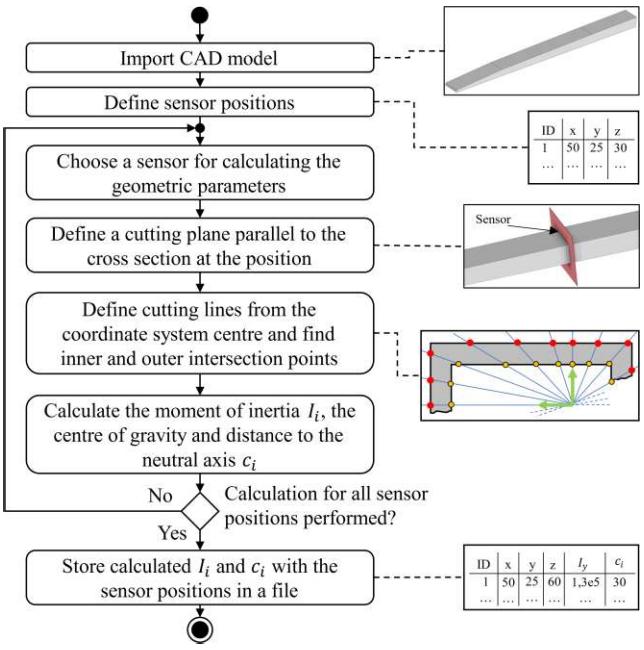

Fig. 2. Procedure of the algorithm to calculate needed geometric parameters from a CAD model at sensor positions for shape sensing.

In the beginning, the geometry of the part is imported from a CAD model. Since the algorithm should not be limited to specific commercial tools, the model has to be in the form of a *.stp file. Afterwards, the user has to specify and define the positions of the sensors, where the geometric parameters second moment of inertia I_i and the distance to the neutral axis c_i at each position i have to be calculated. This calculation is performed in a loop over all the defined sensor positions, until for every of them values of I_i and c_i are calculated. To do so, a plane is defined at each of the sensor positions, which is parallel to the cross-section of the part at one end. In case of Fig. 1, the plane would, for example, always be defined parallel to cross section 1. Due to the defined plane, the CAD model is cut at the desired position. From the position of the two known coordinate axes at the cut, a certain number of lines is defined which will intersect with the considered cross-section of the components CAD model. These intersection points are then clustered into intersections with the outer and the inner parts of a tubular component. All intersection points are then used for a triangulation to approximate the whole area of the part. If there is only one intersection point found for each line, the component is found to be of full-material and the triangles are constructed between the intersection points and the coordinate system's origin. For each triangle, the area and the second moment of area under consideration of Steiner's parallel axis theorem are calculated. Based on this calculation, the centre of gravity is calculated for the whole cross-sectional area. This allows to calculate the distance of the sensor under consideration to the neutral axis. After this procedure is finished for all sensors, the whole data is stored in a file for further processing in the calculation with Ko's displacement theory. Therefore, the second moment of area of the first two sensors closest to the clamped end is used in the first place to estimate the strain at the clamped end because it is difficult to measure there directly [11,14]. So, the strain at this position $i = 0$ is derived from the strain measurements at the sensors with ID 1 and 2 $(i = 1, 2)$, using Equation (1).

$$\varepsilon_0 = I_{y,0}\left[\frac{\varepsilon_2}{I_{y,2}} - (x_2 - x_0)\frac{\left(\frac{\varepsilon_2}{I_{y,2}} - \frac{\varepsilon_1}{I_{y,1}}\right)}{(x_2 - x_1)}\right] \quad (1)$$

With this information, the deformation of the component is calculated using Equation (2) and (3) for Ko's displacement theory for slightly tapered beams or Equation (4) and (5) for tapered beams since (2) and (3) are only applicable for $c_i/c_{i-1} \to 1$.

$$\tan\theta_i = \frac{\Delta l_i}{2 \cdot c_{i-1}}\left[\left(2 - \frac{c_i}{c_{i-1}}\right)\varepsilon_{i-1} + \varepsilon_i\right] + \tan\theta_{i-1} \quad (2)$$

$$w_i = \frac{(\Delta l_i)^2}{6 \cdot c_{i-1}}\left[\left(3 - \frac{c_i}{c_{i-1}}\right)\varepsilon_{i-1} + \varepsilon_i\right] + w_{i-1} + \Delta l_i \tan\theta_{i-1} \quad (3)$$

$$\tan\theta_i = \Delta l_i\left[\frac{\varepsilon_{i-1} - \varepsilon_i}{c_{i-1} - c_i} + \left(\frac{\varepsilon_{i-1}c_i - \varepsilon_i c_{i-1}}{(c_{i-1} - c_i)^2}\right) log\left(\frac{c_i}{c_{i-1}}\right)\right] + \tan\theta_{i-1} \quad (4)$$

$$w_i = (\Delta l_i)^2\left[\frac{\varepsilon_{i-1} - \varepsilon_i}{2(c_{i-1} - c_i)} + \left(\frac{\varepsilon_{i-1}c_i - \varepsilon_i c_{i-1}}{(c_{i-1} - c_i)^3}\right)\left(c_i\, log\left(\frac{c_i}{c_{i-1}}\right)(c_{i-1} - c_i)\right)\right] +$$

$$w_{i-1} + \Delta l_i \cdot \tan\theta_{i-1} \quad (5)$$

In these equations, $\tan\theta_i$ describes the slope of the bending line at sensor position i and w_i describes the deflection at this position. For the calculation of a beam-like structure with a clamped end, the boundary condition $\tan\theta_0 = w_0 = 0$ at the clamped end is applied [13].

4. Case study

To show the applicability and advantages of the proposed approach, a case study on the part depicted in Fig. 1 is presented in the following. The part is made of carbon fibre reinforced plastics (CFRP) with a completely clamped end at cross-section 1. Cross section 4 represents a free end where a bending load of 900 N is applied equally along the width of the part in positive z-direction. To get data on the strains for this load case, it is simulated using FEM with Abaqus Standard/Explicit 2023 solver.

For the shape sensing task, nine strain gauges are assumed to be used. This choice was made since this was the maximal number along one line after an OSP in the 2020 study of Esposito and Gherlone. Furthermore, the strain gauges are aligned on the top surface of the part with the coordinates shown in Table 2 along a constant y-coordinate close to the edge of the component. The choice for positions close to the edge was made because of the results of Esposito and Gherlone 2020 [11] where best results are found close to the edge of a rectangular, tubular component. Besides, the distribution along the x-axis is based on the results from their study, too.

Table 2. Coordinates, strains and geometric parameters for both, the presented algorithm and the plane-based approach, at the strain gauges considered in the case study.

Sensor and geometric information				Algorithm	Planes
ID	x [mm]	ε_i [mm/mm]	$I_{y,i}$ [mm⁴]	c_i [mm]	c_i [mm]
0	0	55.717·10⁻⁵	847.659·10³	30.00	30.00
1	35	-65.224·10⁻⁵	825.225·10³	29.65	29.30
2	95	-80.213·10⁻⁵	787.549·10³	29.05	28.10
3	185	-76.179·10⁻⁵	732.869·10³	28.15	26.30
4	265	-74.933·10⁻⁵	686.096·10³	27.35	24.70
5	495	-73.021·10⁻⁵	561.076·10³	25.05	20.10
6	785	-61.724·10⁻⁵	488.383·10³	23.58	19.66
7	1235	-43.286·10⁻⁵	387.741·10³	21.33	15.16
8	1505	-27.909·10⁻⁵	329.544·10³	19.88	19.76
9	1735	-22.993·10⁻⁵	148.075·10³	14.13	20.76
10	2000	0,0000	31.909·10³	7.62	7.75

For these coordinates, the algorithm described in Section 3 is applied and the resulting geometric parameters are shown in Table 2. Furthermore, the planes depicted in Fig. 1 are used to perform a benchmark of the algorithm and the results for shape sensing to the plane-based approach, where the neutral axis is assumed to be of a constant z-coordinate at the areas of the planes. The sensors with ID 0 and 10 are used to describe the boundary conditions for Ko's displacement theory and have to

be understood as supports for calculation and not as real sensors. In Table 2, the sensor 0 is assumed to be placed directly at the clamped end and the value of ε_0 is calculated in accordance to Equation (1). The sensor with ID 10 as a calculation support is positioned directly at the free end where the bending moment and therefore the strains resulting from bending are zero in accordance to beam theory.

The calculation of the geometric parameters with the proposed algorithm is performed using 1000 lines for finding intersection points. This choice was made since it showed a maximum error of only ≈ 0,05 % to Autodesk Inventor calculation of second moment of inertia while only taking around 1 s for calculation of one cross-section on a computer with an Intel Core i7-1185G7 with 3 GHz and 16 GB RAM.

After estimating the geometric parameters at each sensor position, the data from Table 2 is used for calculations with Equation (2) and (3), or (4) and (5) respectively. To choose between the case of a tapered and a slightly tapered beam, a threshold of $c_i/c_{i-1} = 0.9$ is chosen and the value is checked for each sensor position. Only the calculation at the sensors with ID 9 and 10 required the use of the equations for a tapered beam with the presented approach. In contrast, these equations were used for ID 5 and 7 in the plane-based approach.

The results of the calculations are visualised in Fig. 3, showing the resulting deflections as bending lines along the beam length. To allow a comparison of the approaches besides the visual comparison, the percentage root mean square error (%ERMS) is calculated as in [11] with Equation (6) and will be used in the following.

$$\%ERMS = 100 \cdot \sqrt{\frac{1}{n} \cdot \sum_{i=1}^{n} \left(\frac{w_i - w_i^{ref}}{w_{max}^{ref}} \right)^2} \tag{6}$$

In this equation, w_i^{ref} denotes the FEM reference value at sensor position i, which is compared to the estimated deflection w_i and is weighted by the maximum deflection in the reference solution w_{max}^{ref}.

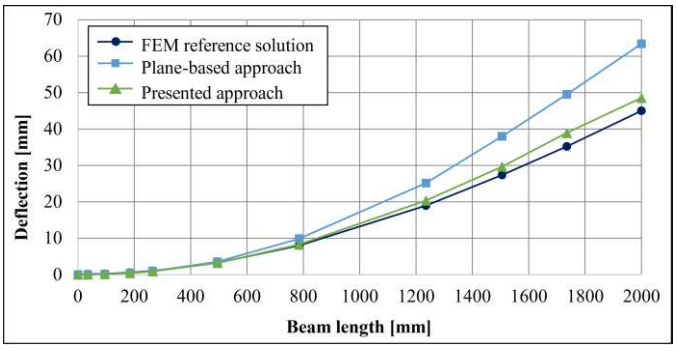

Fig. 3. Results for the two calculation approaches for Ko's displacement theory for tapered beams in comparison to the FEM reference solution.

From the visual comparison of the results, it becomes clear that the plane-based approach and the presented approach yield accurate results at the beginning of the bending lines. However, from the sensor with ID 6 on, the solution with the plane-based approach begins to show greater deviations from the reference solution. The largest deviation can be observed at the free end with a difference of 18.4 mm. Taking not only this value into account but all the calculated results, a %ERMS of 18.55 % is derived with Equation (6). This comparatively high error could be observed because the inaccuracies in the estimation of c_i lead to strong deviations until a new plane section begins. Resulting from this, there is an error propagation due to the consideration of all before calculated values in Equation (2) and (3). However, the results might differ, when there would be more planes defined which would lead to a closer approximation to the results from the presented algorithm. Furthermore, if an OSP had been carried out considering the defined plane sections it might lead to smaller deviations of c_i.

In contrast, the solution with the presented algorithmic approach only starts to show greater deviations beginning at the sensor with ID 8. The maximal deviation is observed at the sensor with ID 9 with 3.68 mm, which shows a good accuracy even without an OSP, which is due to the accurate estimation of c_i, leading to smaller errors. For the presented case study, %ERMS is 4.07 %, which is within the typical range of values for calculations with Ko's displacement theory after an OSP in literature. Therefore, the results of the proposed and presented approach are promising to yield more accurate solutions without assumptions on geometric characteristics after an OSP. Besides, this accuracy enhancement leads to the possibility of finding potential for optimisations of structural components for adaptions on operational loads with enhanced confidence of correct results because of the increase in accuracy.

5. Conclusion and future work

Integrating sensors into structural components allows the acquisition of data on operational loads during the product use phase, which enables the adaption of this "gentelligent" product to these loads due to inheriting this information for optimisations in the next product generation. For the reconstruction of full-field information on deformations and loads from measurements at discrete positions on a component, so-called shape sensing methods are applied. Especially Ko's displacement theory is a suitable method, when beam-like structures under mainly bending loads are considered where only few sensors are available. However, in literature, there are applications presented where assumptions are needed for the calculation when geometries with varying cross sections are considered due to missing information on e. g., the distance of all sensors to the neutral axis of the part. Therefore, a methodology and algorithmic approach is presented to overcome this issue due to the calculation of the needed geometric parameters at each sensor position from a CAD model of the component's geometry. This approach is tested in a case study and showed an enhancement in the accuracy of shape sensing with Ko's displacement theory while only taking short time to calculate the geometric parameters of cross sections with a very good accuracy.

In future works, this algorithm will be implemented in an OSP algorithm, so that sensor positions for shape sensing with Ko's displacement theory will be optimised with consideration

of the exact geometric characteristics of a component at the chosen sensor positions. This will enhance the accuracy of the optimisation process since it will reduce the need to make assumptions when freeform geometries are considered. Therefore, the algorithm will also be applied on the example of an OSP with a beam-like, freeform structure, like for example an aerodynamic profile of an airplane wing or a wind energy turbine blade. Besides, the OSP will not only take the bending direction but all displacement directions into account, to show the applicability for a whole component deformation field. Furthermore, the calculation presented here might be enhanced with the calculation of the operational loads based on the patent of Richards and Ko [15]. This would lead to the estimation of full-field information on deformations and loads which could then be used in the paradigm of technical inheritance for optimisations of structural components in future generations.

References

[1] Behrens B-A, Nyhuis P, Overmeyer L, Bentlage A, Rüther T, Ullmann G. Towards a definition of large scale products. Prod. Eng. Res. Devel. 2014;8(1-2):153–64. doi: 10.1007/s11740-013-0503-1.

[2] Kirchner E, Wallmersperger T, Gwosch T, Menning JDM, Peters J, Breimann R et al. A Review on Sensor - Integrating Machine Elements. Advanced Sensor Research 2024;3(4). doi: 10.1002/adsr.202300113.

[3] Kruse F, Küchenhof J, Gomberg I, Breimann R, Krause D, Kirchner E et al. Identification of Parameter Sets for the Selection of Microelectronic Components for Sensor- Integrating Machine Elements. IEEE Sensors J. 2024;24(7):11174–83. doi: 10.1109/JSEN.2024.3365271.

[4] Heide C von der, Steinmetz J, Schollerer MJ, Hühne C, Sinapius M, Dietzel A. Smart Inlays for Simultaneous Crack Sensing and Arrest in Multifunctional Bondlines of Composites. Sensors (Basel) 2021;21(11). doi: 10.3390/s21113852.

[5] Bergmayr T, Höll S, Kralovec C, Schagerl M. Local residual random forest classifier for strain-based damage detection and localization in aerospace sandwich structures. Composite Structures 2023;304:116331. doi: 10.1016/j.compstruct.2022.116331.

[6] Lachmayer R, Mozgova I, Reimche W, Colditz F, Mroz G, Gottwald P. Technical Inheritance: A Concept to Adapt the Evolution of Nature to Product Engineering. Procedia Technology 2014;15:178–87. doi: 10.1016/j.protcy.2014.09.070.

[7] Lachmayer R, Mozgova I. Technical Inheritance as an Approach to Data-Driven Product Development. In: Krause D, Heyden E, editors. Design Methodology for Future Products: Data Driven, Agile and Flexible. Cham: Springer; 2021, p. 47–64. doi: 10.1007/978-3-030-78368-6_3.

[8] Meyer zu Westerhausen S, Raveendran G, Lauth T-H, Meyer O, Rosemann D, Wawer ML et al. Reliability Assessment of Wireless Sensor Networks by Strain-Based Region Analysis for Redundancy Estimation in Measurements on the Example of an Aircraft Wing Box. Sensors (Basel) 2024;24(13). doi: 10.3390/s24134107.

[9] Meyer zu Westerhausen S, Kyriazis A, Hühne C, Lachmayer R. Design methodology for optimal sensor placement for cure monitoring and load detection of sensor-integrated, gentelligent composite parts. Proc. Des. Soc. 2024;4:673–82. doi: 10.1017/pds.2024.70.

[10] Roy R, Tessler A, Surace C, Gherlone M. Efficient shape sensing of plate structures using the inverse Finite Element Method aided by strain pre-extrapolation. Thin-Walled Structures 2022;180:109798. doi: 10.1016/j.tws.2022.109798.

[11] Esposito M, Gherlone M. Composite wing box deformed-shape reconstruction based on measured strains: Optimization and comparison of existing approaches. Aerospace Science and Technology 2020;99:105758. doi: 10.1016/j.ast.2020.105758.

[12] Gherlone M, Cerracchio P, Mattone M. Shape sensing methods: Review and experimental comparison on a wing-shaped plate. Progress in Aerospace Sciences 2018;99:14–26. doi: 10.1016/j.paerosci.2018.04.001.

[13] Ko WL, Richards WL, van Tran T. Displacement Theories for In-Flight Deformed Shape Predictions of Aerospace Structures. NASA/TP-2007-214612 2007. doi:

[14] Valoriani F, Esposito M, Gherlone M. Shape Sensing for an UAV Composite Half-Wing: Numerical Comparison between Modal Method and Ko's Displacement Theory. Aerospace 2022;9(9):509. doi: 10.3390/aerospace9090509.

[15] Richards WL, Ko WL. PROCESS FOR USING SURFACE STRAIN MEASUREMENTS TO OBTAIN OPERATIONAL LOADS FOR COMPLEX STRUCTURES: United States Patent(US 7,715,994 B1). doi: doi:

[16] Meng Y, Bi Y, Xie C, Chen Z, Yang C. Application of Fiber Optic Sensing System for Predicting Structural Displacement of a Joined-Wing Aircraft. Aerospace 2022;9(11):661. doi: 10.3390/aerospace9110661.

[17] Bruno R, Toomarian N, Salama M. Shape estimation from incomplete measurements: a neural-net approach. Smart Mater. Struct. 1994;3(2):92–7. doi: 10.1088/0964-1726/3/2/002.

[18] Qiu Y, Arunachala PK, Linder C. SenseNet: A Physics-Informed Deep Learning Model for Shape Sensing. J. Eng. Mech. 2023;149(3). doi: 10.1061/JENMDT.EMENG-6901.

[19] Xu C, Cao BT, Yuan Y, Meschke G. Transfer learning based physics-informed neural networks for solving inverse problems in engineering structures under different loading scenarios. Computer Methods in Applied Mechanics and Engineering 2023;405:115852. doi: 10.1016/j.cma.2022.115852.

[20] Ghasemzadeh M, Kefal A. Sensor Placement Optimization for Shape Sensing of Plates and Shells Using Genetic Algorithm and Inverse Finite Element Method. Sensors (Basel) 2022;22(23). doi: 10.3390/s22239252.

[21] Biscotti V, Roy R, Gherlone M. Shape monitoring of morphing wing structures using the inverse Finite Element Method. Computers & Structures 2025;309:107652. doi: 10.1016/j.compstruc.2025.107652.

[22] Esposito M, Gherlone M, Marzocca P. External loads identification and shape sensing on an aluminum wing box: An integrated approach. Aerospace Science and Technology 2021;114:106743. doi: 10.1016/j.ast.2021.106743.

[23] Roy R, Esposito M, Surace C, Gherlone M, Tessler A. Shape Sensing of Stiffened Plates Using Inverse FEM Aided by Virtual Strain Measurements. In: Rizzo P, Milazzo A, editors. European Workshop on Structural Health Monitoring: EWSHM 2022 - Volume 1, 1st ed. Cham: Springer International Publishing; Imprint Springer; 2023, p. 454–463. doi: 10.1007/978-3-031-07254-3_46.